ELSEVIER

Ceramics International 26 (2000) 513–516

CERAMICS
INTERNATIONAL

Effect of helium on radiation damage in a SiC/C composite

Jiachao Chen, Peter Jung*

Institut für Festkörperforschung, Forschungszentrum Jülich, D-52425 Jülich, Germany[1]

Received 30 July 1999; received in revised form 7 September 1999; accepted 21 September 1999

Abstract

In fusion reactor materials relatively large amounts of hydrogen and helium will be produced by nuclear reactions. While in metals and alloys the effect of helium on damage structure and mechanical properties is extensively documented, such information is largely missing in ceramic materials. In the present study a silicon carbide–carbon composite was homogeneously implanted with helium from a cyclotron. The damage microstructure after implantation and after subsequent thermal annealing was investigated by transmission electron microscopy (TEM). Populations of bubbles inside the grains and along grain boundaries are observed, with clear dependence of bubble appearance on the type of boundary. Effects on mechanical properties of SiC/C and of radiation damage on other SiC composites are discussed.

Keywords: A. Implantation; B. Electron microscopy; B. Grain boundaries; D. SiC

1. Introduction

Important considerations for structural materials of future fusion reactors are low nuclear activation and potential for high temperature operation. For plasma facing materials another important demand is low atomic number. All these requests are fulfilled by SiC related materials [1]. One of the problems of pure SiC is its limited fracture toughness and thermal shock resistance. Both properties can be improved, for example in a SiC/C composite by the addition of graphite.

An important question with respect to the application of SiC related materials in fusion reactors is their resistance to radiation damage. Radiation damage results from atomic displacements and nuclear transmutations, including the generation of helium and hydrogen isotopes. Up to now investigations on helium induced microstructural changes were confined to pure SiC, in which helium was either implantated to shallow depth by using helium ions in the keV range (cf. Ref. [2]), or by neutron irradiation of boron doped material (cf. Refs. [3,4]). In the present work, α-particles of energies from 0 to $\approx$25 MeV were implanted homogeneously up to depths of $\approx$250 μm. Therefore, results are not affected by surfaces from shallow implantation or by grain boundaries from boron segregation. After previous studies on irradiation induced changes of dimensional stability [5] and fracture properties [6] of this material, the present work concentrates on microstructural investigations after helium implantation.

2. Experimental details

The SiC/C particulate composite (trade name SiC30, density 2.65 g/cm^3) was supplied by Schunk Kohlenstoff GmbH. Chemical analysis gave an overall composition of 36.7 at% Si and 63.3 at% C. Transmission electron microscopy (TEM) showed mostly β-SiC and some grains of C and few of Si. Most boundaries therefore were β-SiC/β-SiC with some twin boundaries and some Si/β-SiC or C/β-SiC boundaries, while no Si/C boundaries were observed. The graphite had, before implantation, a distorted, partially amorphous appearance with typical morphologies shown in Fig. 1. Also in the graphite, small cavities or even clusters of cavities were observed (Fig. 2). Therefore, a differentiation between pre-existing and implantation induced bubbles was largely impossible in the graphite grains.

Helium implantation was performed at room temperature and at 1000°C at the Compact Cyclotron of

---

* Corresponding author. Tel.: +49-2461-614036; fax: +49-2461-612410.

E-mail address: p.jung@fz-juelich.de (P. Jung).

[1] Association EURATOM-FZJ.

0272-8842/00/$20.00 © 2000 Elsevier Science Ltd and Techna S.r.l. All rights reserved.
PII: S0272-8842(99)00087-5

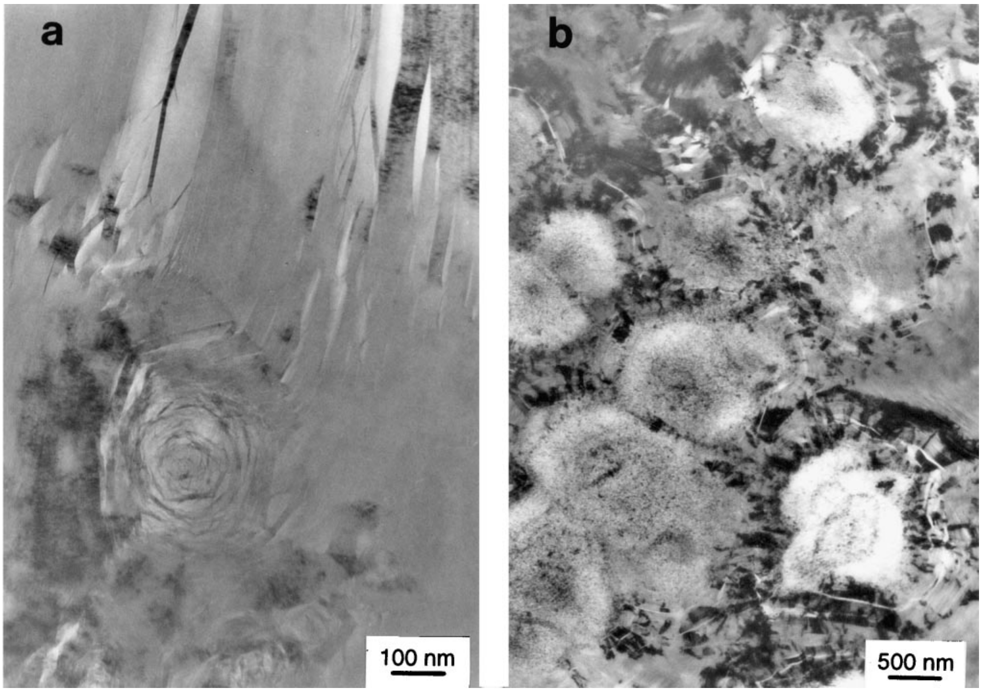

Fig. 1. Morphology of graphite in unirradiated SiC/C, showing (a) layered and (b) flower-like structures.

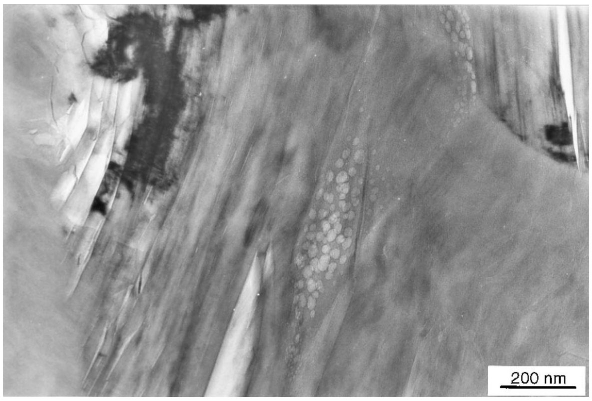

Fig. 2. Clusters of cavities in a graphite grain in SiC/C observed before implantation.

Forschungszentrum Jülich with a 26.3 MeV α-beam which was scanned horizontally and vertically for lateral homogeneity and passed through a 28 μm aluminum window into a vacuum chamber ($\leqslant 10^{-3}$ Pa). In front of the specimens was a degrader wheel with 51 aluminum foils of appropriate thicknesses to give homogeneous distribution up to a maximum depth which could be adjusted from 100 to 250 μm. For room temperature implantation, specimens were soldered with Wood's metal to an insulated copper heat sink, ensuring maximum temperatures of $\leqslant 70$°C during implantation and unmounting.

Beam current was measured electrically on the specimen holder. For high temperature implantation the specimens were thermally insulated from the holder. By controlling the beam current, the temperature in the central part of the specimens was adjusted to 1000°C as monitored by an infrared pyrometer. Average numbers of displaced atoms (N_d), produced in SiC/C per implanted helium atom, range from ≈ 50 for a maximum implantation depth of 100 μm to ≈ 60 for 250 μm. For details of the calculation, compare Ref. [7]. Monte Carlo calculations by TRIM95 gave [8] higher values by about a factor of 1.6.

Specimens for TEM investigations on a Philips TEM430 (300 kV) were dimpled from both sides and perforated by ion milling (Gatan 691 PIPS). This means that the investigated part of the specimens was far away from previous surfaces. Preparation of TEM specimens from SiC/C was rather difficult due to the inhomogeneity of the material. Annealing of specimens was performed in a furnace under vacuum of $\leqslant 10^{-4}$ Pa, always before thinning. The main TEM technique employed was phase contrast for identification of small bubbles.

3. Results

After helium implantation to 1000 atppm at room temperature no bubbles were observed in SiC/C, while bubbles appeared after annealing for 1 h at 1050°C. There was a clear difference between bubbles in grain boundaries and in the grain interiors and there were great differences in bubble appearance, depending on type and orientation of the boundaries. No bubbles were observed on boundaries including graphite grains. In the interior of graphite grains, as already mentioned, some cavities were present before implantation and no significant increase of the number of cavities after implantation was distinguished.

Fig. 3 shows a silicon grain surrounded by SiC grains. Bubbles in silicon grains were only observed for grain sizes above ≈5 μm with typical sizes of 40 nm. Closer observations of Si/Si and Si/SiC boundaries are given in Figs. 4 and 5, respectively. At the Si/SiC boundary the bubbles obviously grow only into the silicon grain. No bubbles were observed after high temperature implantation (1000°C) to 800 atppm at Si/SiC boundaries. In β-SiC/β-SiC boundaries bubbles, extended to both sides (Fig. 6) and were much smaller (≈5–10 nm) than in Si/SiC boundaries (≈100 nm). Their appearance strongly depended on the relative orientation of the adjacent grains. No bubbles were observed in β-SiC twin boundaries as shown in Fig. 7. Inside β-SiC grains, bubbles were very small (≈2 nm), mostly arranged in disks surrounded by strain contrast or attached to dislocations (Fig. 8).

4. Discussion

The most conspicuous microstructural features in the SiC/C composite were the one-sided faceted bubbles at

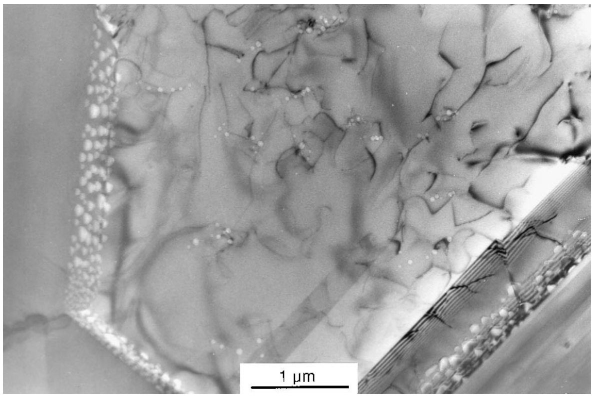

Fig. 3. A silicon grain with boundaries to β-SiC in SiC/C after implantation of 1000 atppm helium at room temperature and annealing at 1050°C for 1 h.

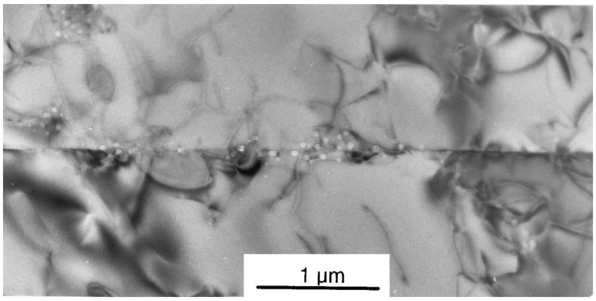

Fig. 4. A Si/Si boundary in SiC/C after implantation of 1000 atppm helium at room temperature and annealing at 1050°C for 1 h.

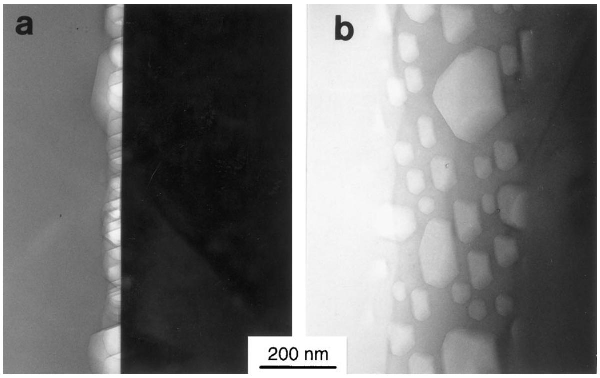

Fig. 5. Bubbles on a boundary separating a Si (left) and a β-SiC grain (right) in SiC/C implanted with 1000 atppm helium at room temperature and annealed for 1 h at 1050°C. The grain boundary is shown (a) edge-on and (b) tilted by 70°.

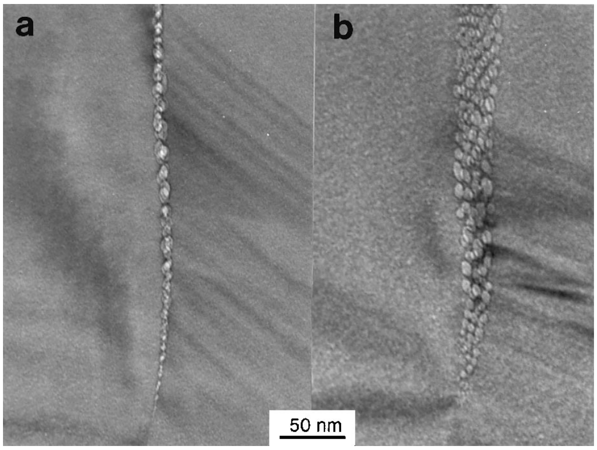

Fig. 6. A β-SiC/β-SiC boundary, (a) edge-on and (b) tilted by 30° after implantation of 1000 atppm helium at room temperature and annealing at 1050°C for 1 h.

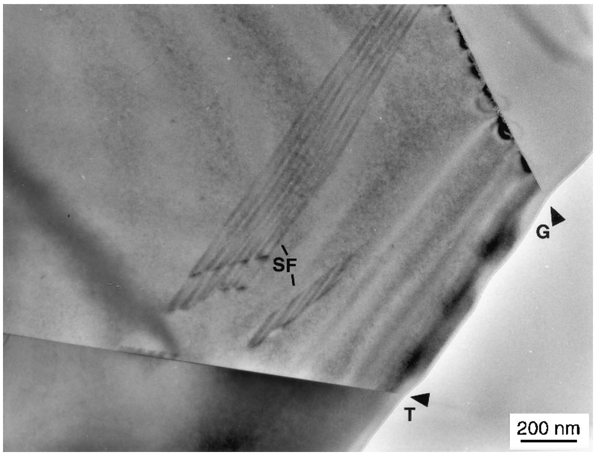

Fig. 7. Twin boundary (T) of β-SiC without bubbles in comparison to a normal grain boundary (G) with helium bubbles in SiC/C after implantation of 1000 atppm helium at room temperature and annealing at 1050°C for 1 h.

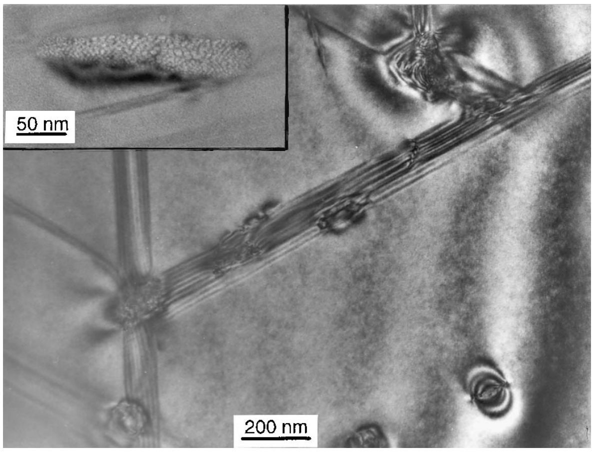

Fig. 8. Bubbles and clusters of bubbles in a β-SiC grain in SiC/C after implantation of 1000 atppm helium at room temperature and annealing at 1050°C for 1 h. The insert shows an enlarged view of a cluster of bubbles.

the Si/SiC interface and the apparent non-occurrence of bubbles in graphite grains and their boundaries. The differences in the occurrence of bubbles in graphite, Si and SiC can be understood by the very different coefficients of helium- and self-diffusion in these materials. Diffusion coefficients of helium at e.g. 1050°C are $\approx 1.7\times10^{-9}$ in graphite [9], 6.8×10^{-10} in Si [10], and 5.0×10^{-11} m^2/s in α-SiC [9], respectively. The high diffusion coefficient can explain why helium disappears from boundaries adjacent to graphite.

Bubble formation during implantation to very high doses already at room temperature and 500°C in graphite, as observed in Ref. [11], is also in agreement with high mobility of helium. Also, the disappearance of helium bubbles at Si/SiC boundaries above 1000°C can be ascribed to the relatively high helium diffusion coefficient in Si. The preferential growth of bubbles into the Si grains at Si/SiC boundaries is probably due to the much higher self diffusion in Si and the correspondingly higher supply of vacancies. At 1050°C self diffusion coefficients in Si are 3.1×10^{-20} [12,13], and in β-SiC (α-SiC) extrapolate to 1.6×10^{-29} (5×10^{-27}) for C [14] and to 8.3×10^{-33} (1.5×10^{-29}) m^2/s for Si [15], respectively.

With respect to mechanical properties of SiC/C, it was found that bending strength σ_B of the virgin material was dominated by the lower strength of the graphite [6]. σ_B was found to be increased by helium implantation up to doses of about $c_s\approx100$ atppm and then was levelling off. As no visible traces of helium were observed in the C-grains, it must be concluded that the increase of σ_B is due to displacement defects in the graphite. The levelling off of σ_B would then be due to saturation of the displacement defects at a reasonable level of $c_s\times N_d\approx0.6\%$.

5. Conclusions

No formation of bubbles in boundaries including graphite grains may indicate potential benefits of SiC-fibre/graphite composites. On the other hand, in SiC/SiC grain boundaries bubbles form at high densities, probably with negative effects on the mechanical properties of SiC_fSiC composites. The role of broad defect free zones, observed along grain boundaries in α-SiC [16], needs further investigation in the case of β-SiC.

References

[1] L.L. Snead, R.H. Jones, A. Kohyama, P. Fenici, J. Nucl. Mater. 233–237 (1996) 26.
[2] K. Hojou, S. Furuno, K.N. Kushita, H. Otsu, K. Izui, J. Nucl. Mater. 191–194 (1992) 583.
[3] S.H. Harrison, J.C. Corelli, J. Nucl. Mater. 122–123 (1984) 833.
[4] T. Suzuki, T. Yano, T. Mori, H. Miyazaki, T. Iseki, Fusion Technol. 27 (1995) 314.
[5] P. Jung, Z. Zhu, J. Chen, J. Nucl. Mater. 251 (1997) 276.
[6] J. Chen, P. Jung, H. Ullmaier, Workshop on Small Scale Testing Techniques, Tougatta Onsen, in preparation.
[7] Z. Zhu, P. Jung, J. Nucl. Mater. 212–215 (1994) 1081.
[8] J.P. Biersack, L.G. Haggmark, Nucl. Instr. Meth. 174 (1980) 257.
[9] P. Jung, J. Nucl. Mater. 191–194 (1992) 377.
[10] P. Jung, Nucl. Instr. Meth. Phys. Res. B91 (1994) 362.
[11] V.N. Chernikov, W. Kesternich, H. Ullmaier, J. Nucl. Mater. 227 (1996) 157.
[12] L. Kalinowski, R. Seguin, Appl. Phys. Lett. 35 (1979) 211.
[13] L. Kalinowski, R. Seguin, Appl. Phys. Lett. 36 (1980) 171.
[14] M.H. Hon, R.F. Davis, J. Mater. Sci. 14 (1979) 2411.
[15] M.H. Hon, R.F. Davis, D.E. Newbury, J. Mater. Sci. 15 (1980) 2073.
[16] J. Chen, P. Jung, PhD thesis, RWTH Aachen, Report Forschungszentrum Jülich, Jül-3585, ISSN 0944-2952, 1998.